In-line Thermal Desorption and Dielectric Barrier Discharge Ionization for Rapid Mass Spectrometry Detection of Explosives

Thomas P. Forbes[1*], Elizabeth L. Robinson[1], Edward Sisco[1], and Abigail Koss[2]

[1]*National Institute of Standards and Technology, Materials Measurement Science Division, Gaithersburg, Maryland 20899, USA*

[2]*TOFWERK USA, Boulder, Colorado 80301, USA*

[*] Corresponding author: TPF: *E-mail:* thomas.forbes@nist.gov

ORCIDs
TPF: 0000-0002-7594-5514
ELR: 0000-0001-8330-2503
ES: 0000-0003-0252-1910
AK: 0000-0002-2415-1730

TOC graphic

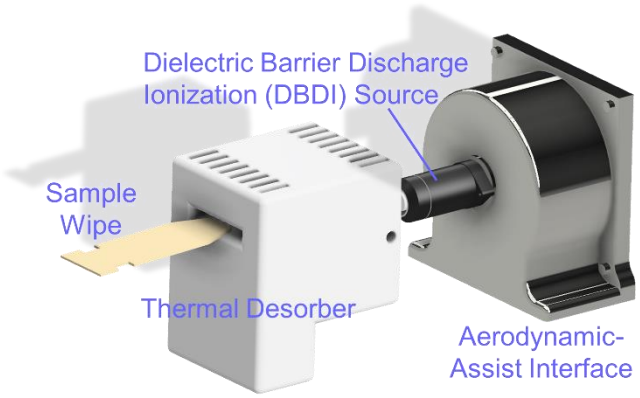

Abstract

Thermal desorption (TD) of wipe-based samples was coupled with an in-line dielectric barrier discharge ionization (DBDI) source and rugged compact time-of-flight mass spectrometer (MS) for the detection of explosives, propellants, and post-blast debris. The chromatography-free TD-DBDI-MS platform enabled rapid and sensitive detection of organic nitramine, nitrate ester, and nitroaromatic explosives, as well as black powder and black powder substitute propellants. Parametric investigations characterized the response to TD temperature, and optimized DBDI voltage, aerodynamically assisted entrainment, and fragmentation through in-source collision induced dissociation (isCID). Excess nitrate generated by the DBDI source yielded predominantly nitrate-adduct formation. Sub-nanogram sensitivities were demonstrated for all explosives investigated, except for nitroglycerin, specifically due to its volatility. Further, most analytes/explosives exhibited tens of picogram sensitivities. The platform also demonstrated the detection of propellant and military explosives from post-blast debris. The TD-DBDI-MS system performed well without the need for aerodynamically assisted entrainment (and the associated rough pump), which along with requiring no additional gasses (*i.e.,* N_2 or He) or solvents, aid in

potential field deployment. The ease of TD-DBDI attachment and removal added trace solid or liquid residue detection to the rugged mass spectrometer, designed primarily for analysis of volatile organic and inorganic compounds.

Keywords: Trace detection; Dielectric barrier discharge ionization; Mass spectrometry; Explosives; Time-of-flight; Propellants; Swipe sampling;

Introduction

Technological advancements have driven development in more ruggedized and portable or transportable instrumentation, enabling traditionally laboratory-based chemical analyses to move into the field or remote arenas. On-site chemical analysis encompasses many applications, including checkpoint screening, crime scene or incident investigations (*e.g.,* industrial or environmental accidents), and environmental monitoring. Rapid compound identification provides near real-time information critical for first responders and/or community safety, as well as for disrupting the movement or entry of hazardous or contraband materials (*e.g.,* explosives, narcotics, restricted/prohibited items).[1] In addition to the range of applications, a range of chemical analysis instrumentation also exists, differing in the chemical properties interrogated or the levels of specificity and sensitivity provided. Colorimetry, vibrational spectroscopy (*i.e.,* Raman and Fourier transform infrared), and ion mobility spectrometry have all seen significant fieldable use for chemical analysis, specifically for drugs, explosives, and hazardous materials (HAZMAT) identification.[2, 3] These analytical techniques are widely deployed for checkpoint screening and infrastructure protection due to their portability, short analysis time, and ease of use.[4, 5]

Advancements in portability have also translated to mass spectrometry.[6] Mass spectrometry (MS) often delivers larger dynamic ranges, enhancements to selectivity and sensitivity, and complex mixture analysis capabilities beyond alternative techniques such as

spectroscopy or ion mobility spectrometry.[7] However, instrumental specifics will ultimately determine the mass resolution and compound differentiation (*e.g.*, time-of-flight [TOF][8] vs high-pressure ion trap mass analyzers[9]) or capabilities to inform on compound structure by tandem mass spectrometry (*e.g.*, ion trap or triple quadrupole vs TOF mass analyzers). Recent years have seen an expansion in fieldable MS solutions for forensic and security sectors,[10] enabled both by advancements in miniaturization and the progression of ambient ionization. Originating in the early 2000s with the advent of direct analysis in real time (DART)[11] and desorption electrospray ionization (DESI),[12] ambient ionization approaches have expanded extensively[13, 14] and been applied to countless applications, including forensics[15, 16] and explosives detection.[17, 18] Recent studies have focused on comparing multiple ambient ionization platforms all on a single mass spectrometer, including atmospheric pressure chemical ionization (APCI), DESI, paperspray ionization (PSI), papercone spray ionization (PCSI), and electrospray ionization (ESI) on a cylindrical ion trap for forensic evidence screening;[16] and ESI, PSI, atmospheric solids analysis probe (ASAP), thermal desorption corona discharge (TDCD), and DART on a single quadrupole for explosives detection.[18]

In this Technical Note, we employ a multimode ambient ionization coupling that enabled rapid chromatography-free analysis of organic explosive, propellant, and post-blast debris mass spectrometry signatures. Thermal desorption (TD) of wipe-based (*i.e.,* from swipe sample collection) and melting point capillary-based (*i.e.,* from liquid extraction) sample introduction was connected in-line with a dielectric barrier discharge ionization (DBDI) source. The TD-DBDI front-end platform was interfaced with a compact transportable time-of-flight mass spectrometer. The rugged mass spectrometer has been deployed extensively for mobile laboratory, point-of-need, and remote field site applications,[19-21] focusing primarily on volatile organic and inorganic compounds (VOCs and VICs). Here, we characterized ion distributions for a series of nitramines, nitrate esters, and nitroaromatics; thermal desorption temperature, DBDI voltage,

aerodynamically-assist entrainment, and fragmentation (*i.e.,* in-source collision induced dissociation: isCID); and performance metrics (*i.e.,* limits of detection) of the TD-DBDI-MS platform. We demonstrated TD-DBDI-MS required no additional gasses (*e.g.,* N_2 or He), solvents, or additional aerodynamically assisting rough pumps for operation, eliminating potential hurdles to field deployment. The front-end also expanded the utility of the TOF mass spectrometer, developed primarily for vapor-phase monitoring, to trace solid- and liquid-phase samples.

Methods

Materials. Organic explosive standards for nitramines: 1,3,5-trinitroperhydro-1,3,5-triazine (RDX) and 1,3,5,7-tetranitro-1,3,5,7-tetrazocane (HMX or octogen), nitrate esters: pentaerythritol tetranitrate (PETN) and nitroglycerin (NG), and nitroaromatics: trinitrotoluene (TNT) and (2,4,6-trinitrophenyl)methylnitramine (Tetryl) were purchased from AccuStandard Inc. (New Haven, CT, USA) at 1 mg/mL in acetonitrile. Standards were gravimetrically diluted in liquid chromatography (LC)-MS Chromasolv grade acetonitrile (Sigma-Aldrich, St. Louis, MO, USA) for further use. Single component standard dilutions were directly deposited onto sampling wipes (polytetrafluoroethylene (PTFE)-coated fiberglass weave wipes, DSA Detection, LLC, Boston, MA, USA). Black powder and black powder substitute propellants and post-blast debris were also swipe sampled and analyzed. Composition details can be found in the supporting information.

Instrumentation. Thermal desorption (TD) of wipe-based samples was conducted with a resistance-based heater held at constant temperature.[22, 23] The desorber was coupled to an in-line dielectric barrier discharge ionization (DBDI) source (SICRIT [soft ionization by chemical reaction in transfer], Plasmion GmbH, Augsburg, Germany),[24] mounted on the inlet of Vocus S compact time-of-flight mass spectrometer (TOFWERK AG, Thun, Switzerland/TOFWERK USA, Boulder, CO, USA). The mass spectrometer was fitted with an atmospheric pressure interface adapting flange to provide aerodynamic-assist with an associated rough pump to enhance flow

rates toward the inlet. The DBDI source incorporated a concentric electrode flow-through geometry, with the thermal desorber and ambient air on one end, and the aerodynamic-assist interface and MS inlet on the other.[25, 26] The pull of ambient air through the thermal desorber led to the generation of background nitrate species in negative mode mass analysis. Further details of the DBDI source can be found in the literature.[24-27] Analyte vapors were generated and ionized within the front-end (*i.e.,* thermal desorber – DBDI source – aerodynamic-assist interface), traveled through a series of RF-only quadrupole ion guides (short segmented quadrupole [SSQ] and big segmented quadrupole [BSQ]), accelerated orthogonally through a reflectron TOF, and detected by a multichannel plate. Fragmentation was achieved by in-source collision induced dissociation (isCID), applied in the differentially pumped region between the skimmer and BSQ, just downstream of the SSQ. Mass spectra were collected from *m/z* 8 to *m/z* 800 at 10 Hz spectral rate. Additional details of supporting instrumentation, measurements, and methods can be found in the electronic supporting information.

Safety Considerations. Best practices and material safety data sheet recommendations were followed for storage and handling of energetic materials. A portable fume extractor with HEPA and carbon filters was used during experiments with thermal desorption to capture potential aerosol or vapor release.

Data Availability. Raw data files, extracted mass spectra, and derived data files are available on the NIST Public Data Repository: https://doi.org/10.18434/mds2-3299.

Results and Discussion

The coupling of TD-DBDI with a rugged time-of-flight mass spectrometer (Figure 1(a)) was explored for the analysis of wipe-based and swipe sampled explosives, propellants, and post-blast debris. Mass spectral signatures, fragmentation patterns, and performance metrics were measured for pairs of each nitramine (*i.e.,* RDX and HMX), nitrate ester (*i.e.,* PETN and NG), and

nitroaromatic (*i.e.,* TNT and Tetryl) explosives. The DBDI source generated significant nitrate anion in negative mode MS – as well as a smaller abundance of the nitrate dimer $[(HNO_3)NO_3]^-$. The background mass spectrum closely resembled similar plasma-based sources (*e.g.,* DART [with N_2] or corona discharge). The nitrate-based explosives predominately formed nitrate-adducts, with the main observed ion for each listed in Table 1. Figure 1(b) displays the full scan mass spectrum for RDX, demonstrating the nitrate-adduct (*m/z* 284 $[RDX+NO_3]^-$) and some bare nitrate anion (full scan spectra for all compounds can be found in supporting information, Figure S1). At the low mass loadings investigated, no significant dimer peaks (or other peaks) in the high(er) ion mass range (*i.e., m/z* >400) were observed, therefore displayed spectra were generally truncated at *m/z* 400. The only deviation from nitrate adducts was observed for the nitroaromatic TNT, where the common loss of -NO was observed (*m/z* 197 $[TNT-NO]^-$) and adduct (*m/z* 260 $[TNT+OOH]^-$) previously observed with DART and APCI[18, 28] (Figure 1(c)). Interestingly, Tetryl also yielded predominantly the nitrate adduct (*m/z* 349 $[Tetryl+NO_3]^-$), with minor peaks for the loss of NO and NO_2 (Figure S1). Previous works with related plasma-based sources such as DART, confined DART, ASAP, and TDCD exhibited the *m/z* 241 $[Tetrly-NO_2]^-$ (N-methyl-2,4,6 trinitroaniline fragment ion) as the dominant observed ion.[18, 29, 30] Ion distributions were also briefly investigated on an alternative mass analyzer (JEOL AccuTOF time-of-flight) to gauge ion source vs mass analyzer effects (Figure S2). There was very little difference observed for most of the explosives investigated. Minor differences in the relative ratios of fragments to nitrate adduct of Tetryl and TNT were observed, though a more detailed comparison would be required to eliminate any other effects.

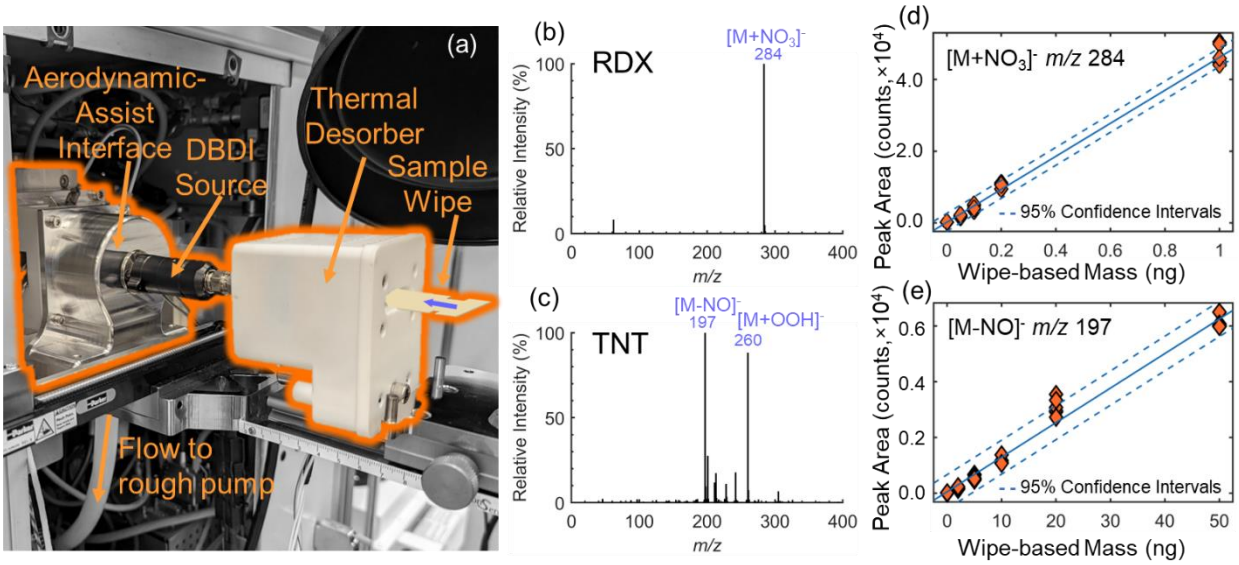

Figure 1. (a) Image of the TD-DBDI-MS (inlet) configuration and main front-end components – wipe-based sample introduction, thermal desorber, DBDI source, and aerodynamic-assist interface. Exemplar mass spectra for (b) RDX and (c) TNT samples measured from PTFE-coated fiberglass weave wipes. Low sample mass response curves for (d) RDX and (e) TNT from replicate measurements (n=6 at each wipe-based loading), with linear fit and 95% confidence intervals.

Sensitivity of the TD-DBDI-MS platform was investigated by low mass loading response curves (Figures 1(d-e) and S3) and the ASTM E2677 Standard Test Method for Determining Limits of Detection in Explosive Trace Detectors.[31] Single-component analytical standards in acetonitrile were serially diluted and 2 µl deposited onto PTFE-coated fiberglass weave wipes, allowing the solvent to evaporate. Target ion peaks for each compound were integrated from extracted ion chronograms. Blank controls consisted of 2 µl blank acetonitrile. The ASTM E2677 method results are displayed in Table 1 and correspond to the wipe-based mass that resulted in 90 % probability of true detection. Most compounds exhibited sub-nanogram detection limits, with many in the tens of picograms range. However, NG demonstrated an LOD_{90} on the order of tens of nanograms. The poorer performance of NG was attributed to the compound's higher volatility (relative to the others) and a sub-optimal thermal desorption temperature (250 °C). A more detailed characterization of the thermal desorption temperature follows below.

Table 1. TD-DBDI-MS analysis of organic explosives, including dominant observed ion(s) and LOD_{90} values (calculated according to ASTM E2677[31]). Sensitivity measurements were collected with a 250 °C thermal desorption temperature, and aerodynamic-assist of 0.8 L/min (*i.e.,* 200 steps valve reading), and DBDI settings of 1400 V and 15 kHz.

Compound	Vapor Pressure at 25°C (kPa)[32]	*m/z*	Observed Ion	Wipe LOD_{90} (ng)
HMX	2.40×10^{-15}	358.16	$[HMX+NO_3]^-$	0.02
RDX	4.91×10^{-10}	284.12	$[RDX+NO_3]^-$	0.01
TNT	9.27×10^{-7}	197.12 260.12	$[TNT-NO]^-$ $[TNT+OOH]^-$	0.65 0.50
Tetryl	1.60×10^{-8}	349.15	$[Tetryl+NO_3]^-$	0.04
PETN	1.08×10^{-9}	378.14	$[PETN+NO_3]^-$	0.02
NG	6.54×10^{-5}	289.09	$[NG+NO_3]^-$	23.1

The TD-DBDI-MS system response to TD temperature demonstrated trends that varied by compound, similar to previous works using similar wipe-based heating platforms.[23, 33] Specifically, optimal TD temperatures were primarily dependent on the compound's volatility (correlating with vapor pressure – Table 1). Figure 2(a) displays the integrated peak areas for 20 ng NG and 2 ng HMX (the two extremes of vapor pressure studied here) as a function of increasing TD temperature. The volatile NG exhibited a tight range of optimal temperature in the lower range explored, around 180 °C. Even at this temperature, the NG temporal profile was very short as demonstrated by the extracted ion chronograms (Figure 2(a-i)). Alternatively, the less volatile explosive, HMX, displayed a broad optimum temperature at high(er) temperatures in the range of 200 °C to 275 °C (Figure 2(a)). At reduced temperatures, the HMX temporal profiles (Figures 2(a-i) and 2(a-ii)) demonstrated slower vaporizing and detection, extending for nearly 30 seconds. This desorption profile was shortened to under 10 s at 250 °C (Figure 2(a-iii)). The hurdles arising from the thermal desorption of energetic compounds with such a great range in volatility has been well documented.[33, 34] These can range from high vapor pressures such as ethylene glycol dinitrate (EGDN), 1.03×10^{-2} kPa,[32] down to exceedingly low vapor pressures of

potassium chlorate and perchlorate oxidizers, estimated at orders of magnitude lower than HMX.[35] Variations in volatility of compounds can be addressed by a range of alternatives, for example, ramped or multistage thermal desorption,[34] areas of future work.

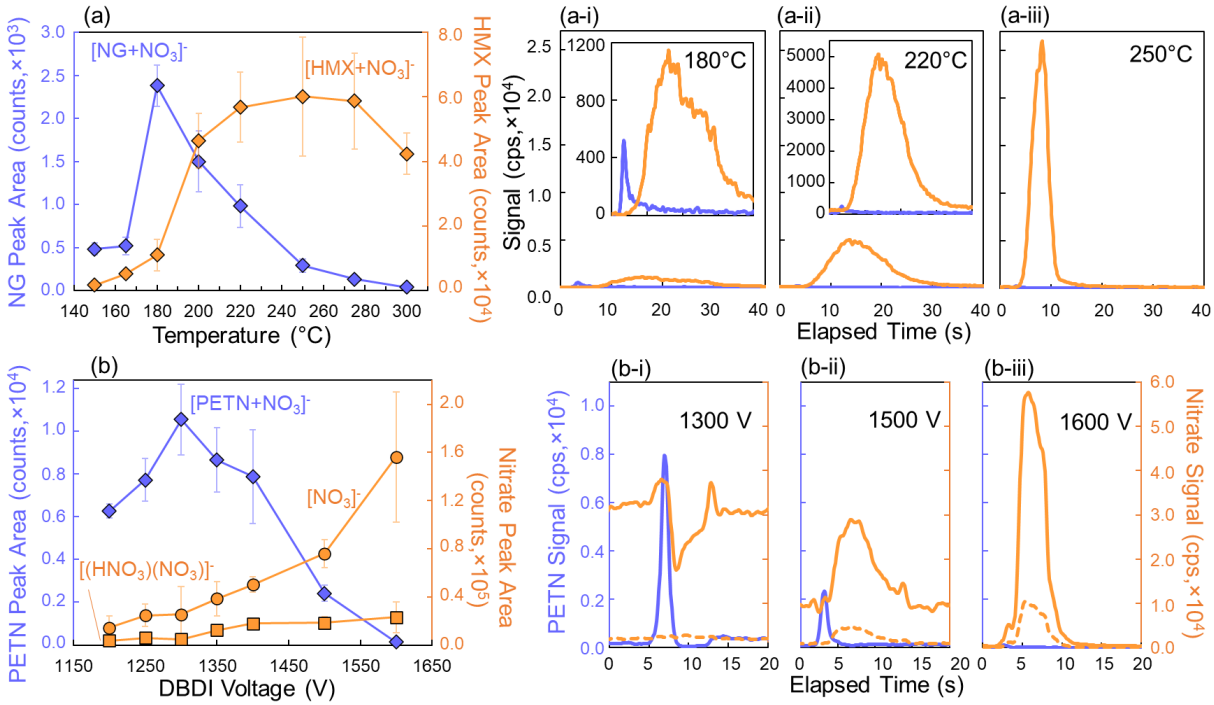

Figure 2. (a) TD-DBDI-MS response of NG (20 ng, blue diamond) and HMX (2 ng, orange diamond) as a function of increasing thermal desorption temperature. Temporal response (extracted ion chronograms) of NG (blue) and HMX (orange) thermal desorption at (a-i) 180 °C, (a-ii) 220 °C, and (a-iii) 250 °C. (b) TD-DBDI-MS response to 0.4 ng PETN (displaying PETN: blue diamonds, nitrate: orange circles, and nitrate dimer: orange squares) as a function of increasing DBDI voltage (all at 15 kHz, 225 °C, and aerodynamic-assist 0.8 L/min). Temporal response (extracted ion chronograms) of PETN (blue), nitrate (solid orange), and the nitrate dimer (dashed orange) at (b-i) 1300 V, (b-ii) 1500 V, and (b-iii) 1600 V. Data points and uncertainty represented by the average and standard deviation of 5-6 replicate samples.

Thermally desorbed compounds in the vapor phase were then entrained through the DBDI region (Figure 1(a)). A minimal electric potential was required to ignite and sustain the DBDI discharge. This minimum ignition voltage was also observed to be a function of the gas flow through the source. The system response of wipe-based PETN samples (0.4 ng) for increasing

DBDI voltage was characterized and displayed in Figure 2(b). The PETN-nitrate adduct peak area increased for the first 100V – 200V above the ignition voltage, followed by a sharp decrease as the DBDI energy sufficiently fragmented PETN. This fragmentation was also observed by the increase in nitrate and nitrate dimer signal during the wipe-based sample introduction (Figure 2(b)). The sample-based nitrate signal demonstrated the opposite trend to the background DBDI-generated nitrate signal (Figure S4). The background nitrate demonstrated a similar trend to PETN that yielded an initial increase in nitrate generation for 100V-200V increase in voltage beyond ignition; followed, by decreased in nitrate (an all background) signal for further increase. At the highest DBDI voltages investigated, the plasma was unstable and nearly all the PETN was fragmented to bare nitrate anions.

The DBDI ignition voltage and stability range was directly affected by the gas flow rate through the plasma region. In this configuration of the TD-DBDI-MS platform, the aerodynamic-assist interface coupling the DBDI source to the MS inlet managed the gas flow rate. Similar aerodynamic-assist interfaces were introduced for DART ion sources to separate excess helium from entering the mass spectrometer,[36] as well as providing entrainment through confined geometries.[23] An external rough pump was connected to the aerodynamic-assist chamber (Figure 1(a)) and flow rate controlled through a valve with variable orifice, opening and closing by ‘steps’. A roughly exponential relationship between steps and flow rate through exhaust pump was observed. Figure 3(a) displays the response to wipe-based RDX samples (2 ng) for no aerodynamic-assist up to approximately 2.5 L/min (*i.e.,* pump valve setting of 300 steps). In the region around 2.5 L/min and greater, the pull was sufficient to extinguish the DBDI plasma, eliminating ionization and signal. The straight flow path from thermal desorber through in-line DBDI source to MS inlet exhibited minimal flow resistance and an optimal RDX signal with no additional assisted pull (Figure 3(a)). The instrument pull from the differentially pumped region through the inlet adequately entrained vaporized wipe-based samples. The trade-off between

removing an additional rough pump and the benefits to peak shape by having a small assisted-pull with minimal loss of signal must be weighed for each specific application. In addition, sample substrate and introduction must be considered. A common alternative to swipe sampling and wipe-based sample introduction incorporates glass melting point capillary tubes for sampling extracted analytes. The thermal desorption of capillary-based samples was achieved with a gas chromatography (GC)-interface heater coupled to the DBDI source (Figure 3(b)). In this geometry, the sample-laden capillary was inserted vertically into the GC-interface heater. Heated gas flow through the GC-interface heater made a 90° turn through the DBDI source and into the mass spectrometer. Figure 3(a) displays the same analysis for capillary-based PETN samples using the GC-interface heater. The larger flow resistance due to the narrow inner diameter and 90° turn yielded an optimal signal for an aerodynamic-assist of 0.9 L/min.

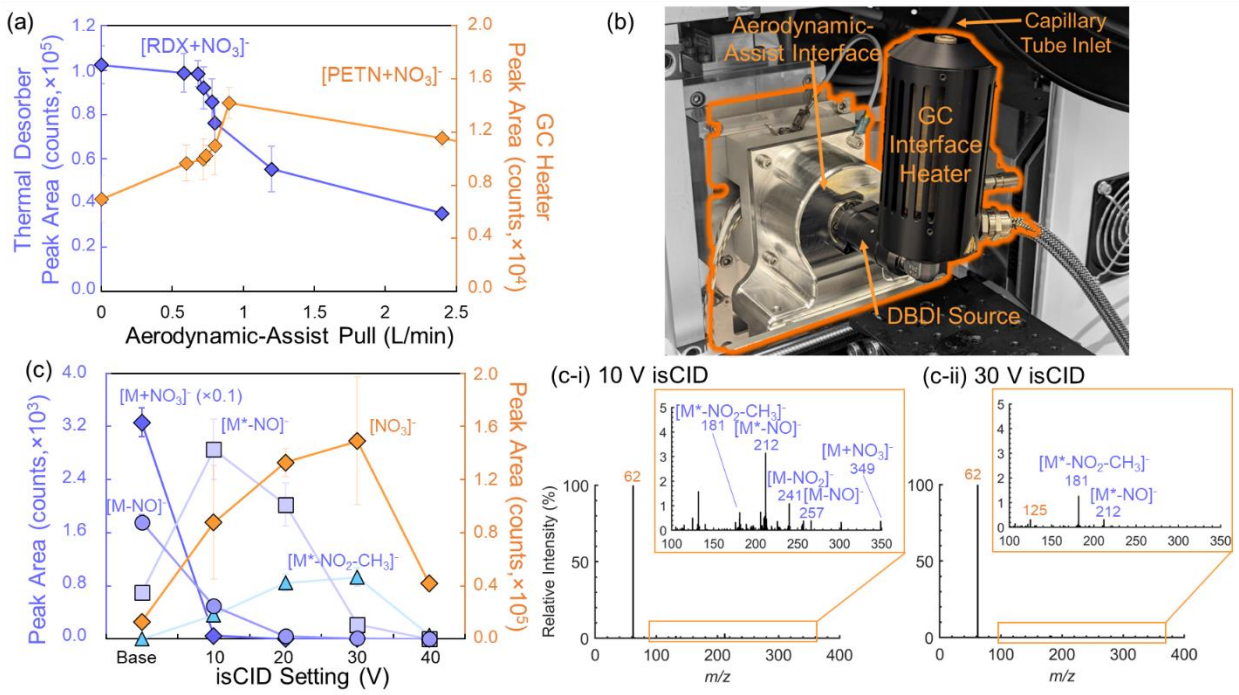

Figure 3. (a) TD-DBDI-MS response to 2 ng wipe-based RDX (blue diamonds) and 1 ng capillary tube-based PETN (orange diamonds) as a function of increasing aerodynamic-assist gas flow (all at DBDI 1300V / 15 kHz). (b) Image of the TD-DBDI-MS (inlet) configuration with alternative GC interface heater. (c) TD-DBDI-MS response to 2 ng wipe-based Tetryl as a function of increasing fragmentation (all at DBDI 1300V / 15 kHz, 225 °C, and 0.8 L/min). Curves represent peak areas for the Tetryl-nitrate adduct (blue diamonds, *m/z* 349) and fragments at *m/z* 257 (circles), *m/z* 212 (squares), *m/z* 181 (triangles), and *m/z* 62 nitrate (orange diamonds). Representative mass

spectra for (c-i) 10 V isCID and (c-ii) 30 V isCID display relative fragment distributions. “M” represents the Tetryl molecule ($C_7H_5N_5O_8$) and “ M* ” the degradation product, N-methylpicramide ($C_7H_6N_4O_6$). Data points and uncertainty represented by the average and standard deviation of 5-6 replicate samples.

With a characterization of the overall instrument and front-end sampling, ionization, and inlet flow, we next considered a brief characterization of compound fragmentation. The TOF mass analyzer used here did not possess tandem mass spectrometry capabilities. However, broad-band fragmentation was achieved by isCID, a technique demonstrated in the literature for declustering[37] and fragmentation to enhance signal,[38] detect inorganic oxidizers,[39, 40] and develop multi-spectra library search algorithms.[41] Fragmentation ion distributions of Tetryl (2 ng wipe-based samples) were investigated for increasing isCID potential (*i.e.,* the voltage difference between the skimmer [between the SSQ and BSQ] and BSQ). All voltages upstream of the skimmer were also similarly adjusted to maintain a roughly equivalent potential gradient. Figure 3(c) displays the peak areas for a few of the main ions and fragments. Here, M and M* represented the Tetryl molecule ($C_7H_5N_5O_8$) and the degradation product N-methylpicramide ($C_7H_6N_4O_6$), respectively. The 10 V isCID settings led to significant fragmentation of Tetryl, nearly eliminating the intact nitrate adduct, as well as larger fragments such as *m/z* 257 $[M\text{-}NO]^-$ and *m/z* 241 $[M\text{-}NO_2]^-$. The interplay between nitrate generated by the DBDI source and nitrate due to fragmentation of nitro-based explosives convoluted its origin. Other than nitrate, the *m/z* 212 $[M^*\text{-}NO]^-$ fragment was the most intense at 10 V isCID (Figure 3(c-i)). Further increase in voltage and fragmentation transitioned the dominant fragment to *m/z* 181 $[M^*\text{-}NO_2\text{-}CH_3]^-$ (Figure 3(c-ii)) and eventually led to fragmentation of all species, including nitrate (isCID 40 V). Overall, the 10 V isCID setting was sufficient to fragment most of the explosives investigated here down to bare nitrate anions (Figure S5). HMX did not show the same level of fragmentation until 20 V and TNT yielded predominantly the loss of NO fragment at 10 V isCID.

Finally, we demonstrate the analysis of more complex samples of interest, including propellants and post-blast debris. In addition to the more traditional military grade explosives, the identification of homemade explosive components remains important. Low-order explosives based on propellants, pyrotechnics, and rudimentary fuel-oxidizer mixtures often fall at the top of the list of explosive device main charges in the annual review by the U.S. Bureau of Alcohol, Tobacco, Firearms, and Explosives (ATF).[42] Figure 4 displays the TD-DBDI-MS signatures for a black powder (Figure 4(a)) and black powder substitute (Figure 4(b)), swipe collected from crushed propellant particles and thermally desorbed at 250 °C. At these desorption temperatures, the black powder (potassium nitrate/sulfur/carbon) exhibited an ion distribution primarily for the more volatile sulfur component (relative to potassium nitrate). Peak assignments were cursory and based on previous work and the literature, including *m/z* 80 S_2O^-, *m/z* 97 HSO_4^-, *m/z* 112 S_3O^-, and *m/z* 195 $[H_2SO_4+HSO_4]^-$.[40, 43] The black powder substitute, Blackhorn 209, exhibited an ion distribution dominated by nitrate-species and guanidine nitrate species (Figure 4(b)). This particular propellant has previously demonstrated two particle distributions, one based on guanidine nitrate/potassium perchlorate and the other on traditional black powders – potassium nitrate/sulfur/carbon.[44] Previous works incorporating high temperature thermal desorption have detected the potassium perchlorate component of Blackhorn 209 as well.[40]

Figure 4 also displays the mass spectra from swipe sampling of post-blast debris from thermoplastic polymer pipe-based explosives devices. These devices were created using fused deposition modeling (FDM), packed with various charges (e.g., dynamite, black powder, and an emulsion explosive), and detonated by heated wire. In this instance, post-blast debris was collected and returned to the laboratory setting for analysis. Figure 4(c) displays clear peaks for the nitrate anion, RDX, HMX, and a polymer distribution. The dynamite charge was primarily composed of TNT and RDX. The lack of TNT signal was not surprising given its volatility and propensity for degradation (samples have been stored in sealed bags away from light since

detonation in 2017).[45] Similarly, HMX is a known byproduct from hexamine nitration for the manufacture of RDX (*e.g.,* the Bachmann process[46]). The more abundant debris from a black powder charge exhibited the expected signals for nitrate and sulfur related species (Figure 4(d)). This corroborated previous analysis of these samples by a counter-flow capillary electrophoresis technique.[44] The Dyno AP charge debris spectrum was dominated by the nitrate dimer (Figure S6), matching previous electrophoresis analysis[44] and aligning with the multiple nitrate species composing the emulsion charge.

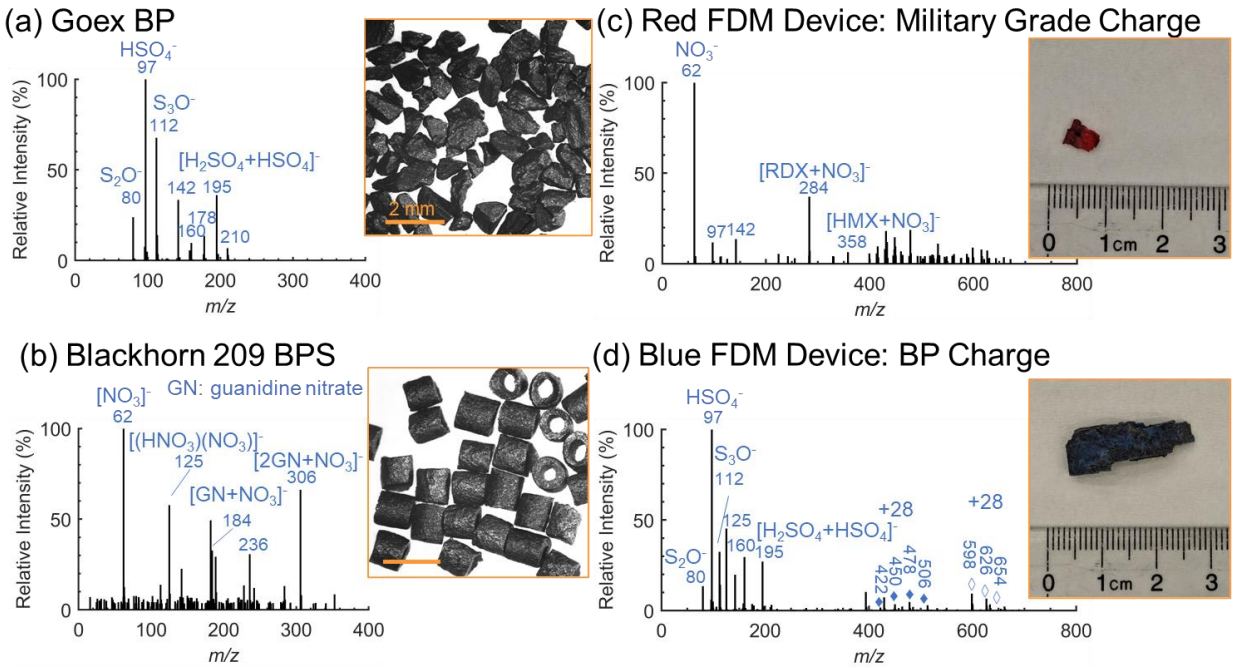

Figure 4. TD-DBDI-MS analysis of propellants swipe collected from crushed particles and post-blast debris of thermoplastic polymer devices. Mass spectra represent (a) Goex black powder and (b) Blackhorn 209 black powder substitute propellants, and post-blast debris from main charges of (c) military dynamite and (d) Schuetzen black powder.

Conclusions

This investigation demonstrated promising capabilities for coupling swipe sampling with TD-DBDI and a rugged mass spectrometer for field screening and investigation applications. This

Technical Note focused on explosives detection, however avenues into the detection of drugs, related contraband materials, and other compounds of interest to forensics and public health are ongoing. Without the need for additional gas cylinders, solvents, or entrainment assisting pumps, the wipe-based TD-DBDI front-end platform established a path to field deployment. Opportunities also exist to couple with smaller or more portable TOF, single quadrupole, or ion trap mass spectrometers. Though sub-nanogram sensitivities were exhibited for most of the explosives tested, these were for pure analytical standards in ideal conditions. Performance in a fielded scenario, with real-world samples and potential background interferences or other matrix effects, may differ significantly. Future work will explore the analysis of complex mixtures and competitive ionization in more detail. In addition, this and related platforms will be adapted for a mobile laboratory setting for on-site chemical analysis, introducing investigations into the effects of environmental conditions (*e.g.,* ambient temperature and humidity), sample collection and preparation, and near real-time sample collection and library matching.

Supporting Information

Additional experimental method details, mass spectra, and figures as noted in the text can be found in the online supporting information.

Acknowledgments

The authors declare no competing financial interests.

The authors would like to thank Cindy Wallace at the Bureau of Alcohol, Tobacco, Firearms, and Explosives for the black powders and black powder substitutes; and Matthew Staymates, Jessica Staymates, and Greg Gillen at NIST for the post-blast debris. The U.S. Department of Homeland

Security Science and Technology Directorate sponsored a portion of the production of this material under Interagency Agreement IAA 70RSAT21KPM000083 with the National Institute of Standards and Technology.

Notes

† Certain commercial equipment, instruments, or materials are identified in this article in order to specify the experimental procedure adequately. Such identification is not intended to imply recommendation or endorsement by NIST, nor is it intended to imply that the materials or equipment identified are necessarily the best available for the purpose.

‡ Official contribution of the National Institute of Standards and Technology; not subject to copyright in the United States.

References

(1) Forbes, T. P.; Burks, R. Field-Deployable Devices. In *Encyclopedia of Forensic Sciences, Third Edition (Third Edition)*, Houck, M. M. Ed.; Elsevier, 2023; pp 413-423.
(2) Yinon, J. Field detection and monitoring of explosives. *TrAC Trends in Analytical Chemistry* **2002**, *21* (4), 292-301. DOI: https://doi.org/10.1016/S0165-9936(02)00408-9.
(3) To, K. C.; Ben-Jaber, S.; Parkin, I. P. Recent Developments in the Field of Explosive Trace Detection. *ACS Nano* **2020**, *14* (9), 10804-10833. DOI: 10.1021/acsnano.0c01579.
(4) Buryakov, I. A. Detection of explosives by ion mobility spectrometry. *Journal of Analytical Chemistry* **2011**, *66* (8), 674. DOI: 10.1134/S1061934811080077.
(5) Mäkinen, M.; Nousiainen, M.; Sillanpää, M. Ion spectrometric detection technologies for ultra-traces of explosives: A review. *Mass Spectrometry Reviews* **2011**, *30* (5), 940-973. DOI: 10.1002/mas.20308.
(6) Snyder, D. T.; Pulliam, C. J.; Ouyang, Z.; Cooks, R. G. Miniature and Fieldable Mass Spectrometers: Recent Advances. *Analytical Chemistry* **2016**, *88* (1), 2-29. DOI: 10.1021/acs.analchem.5b03070.
(7) Brown, H. M.; McDaniel, T. J.; Fedick, P. W.; Mulligan, C. C. The current role of mass spectrometry in forensics and future prospects. *Analytical Methods* **2020**, *12* (32), 3974-3997, 10.1039/D0AY01113D. DOI: 10.1039/D0AY01113D.
(8) Brais, C. J.; Ibañez, J. O.; Schwartz, A. J.; Ray, S. J. RECENT ADVANCES IN INSTRUMENTAL APPROACHES TO TIME-OF-FLIGHT MASS SPECTROMETRY. *Mass Spectrometry Reviews* **2021**, *40* (5), 647-669. DOI: https://doi.org/10.1002/mas.21650.
(9) Blakeman, K. H.; Miller, S. E. Development of High-Pressure Mass Spectrometry for Handheld and Benchtop Analyzers. In *Portable Spectroscopy and Spectrometry*, 2021; pp 391-413.
(10) Evans-Nguyen, K.; Stelmack, A. R.; Clowser, P. C.; Holtz, J. M.; Mulligan, C. C. Fieldable Mass Spectrometry for Forensic Science, Homeland Security, and Defense Applications *Mass Spectrometry Reviews* **2021**, *https://doi.org/10.1002/mas.21646*. DOI: https://doi.org/10.1002/mas.21646.
(11) Cody, R. B.; Laramée, J. A.; Durst, H. D. Versatile New Ion Source for the Analysis of Materials in Open Air under Ambient Conditions. *Analytical Chemistry* **2005**, *77* (8), 2297-2302. DOI: 10.1021/ac050162j (acccessed 2012/11/16).

(12) Takáts, Z.; Wiseman, J. M.; Gologan, B.; Cooks, R. G. Mass Spectrometry Sampling Under Ambient Conditions with Desorption Electrospray Ionization. *Science* **2004**, *306* (5695), 471-473. DOI: 10.1126/science.1104404.
(13) Monge, M. E.; Harris, G. A.; Dwivedi, P.; Fernandez, F. M. Mass Spectrometry: Recent Advances in Direct Open Air Surface Sampling/Ionization. *Chemical Reviews* **2013**, *113* (4), 2269-2308, Review. DOI: 10.1021/cr300309q.
(14) Rankin-Turner, S.; Sears, P.; Heaney, L. M. Applications of ambient ionization mass spectrometry in 2022: An annual review. *Analytical Science Advances* **2023**, *4* (5-6), 133-153. DOI: https://doi.org/10.1002/ansa.202300004.
(15) Sisco, E.; Forbes, T. P. Forensic applications of DART-MS: A review of recent literature. *Forensic Chemistry* **2021**, *22*, 100294. DOI: https://doi.org/10.1016/j.forc.2020.100294.
(16) Lawton, Z. E.; Traub, A.; Fatigante, W. L.; Mancias, J.; O'Leary, A. E.; Hall, S. E.; Wieland, J. R.; Oberacher, H.; Gizzi, M. C.; Mulligan, C. C. Analytical Validation of a Portable Mass Spectrometer Featuring Interchangeable, Ambient Ionization Sources for High Throughput Forensic Evidence Screening. *Journal of The American Society for Mass Spectrometry* **2017**, *28* (6), 1048-1059, journal article. DOI: 10.1007/s13361-016-1562-2.
(17) Forbes, T. P.; Sisco, E. Recent advances in ambient mass spectrometry of trace explosives. *Analyst* **2018**, *143* (9), 1948-1969, 10.1039/C7AN02066J. DOI: 10.1039/C7AN02066J.
(18) Mathias, S.; Amerio-Cox, M.; Jackson, T.; Douce, D.; Sage, A.; Luke, P.; Sleeman, R.; Crean, C.; Sears, P. Selectivity of Explosives Analysis with Ambient Ionization Single Quadrupole Mass Spectrometry: Implications for Trace Detection. *Journal of the American Society for Mass Spectrometry* **2024**, *35* (1), 50-61. DOI: 10.1021/jasms.3c00305.
(19) Gkatzelis, G. I.; Coggon, M. M.; McDonald, B. C.; Peischl, J.; Gilman, J. B.; Aikin, K. C.; Robinson, M. A.; Canonaco, F.; Prevot, A. S. H.; Trainer, M.; et al. Observations Confirm that Volatile Chemical Products Are a Major Source of Petrochemical Emissions in U.S. Cities. *Environmental Science & Technology* **2021**, *55* (8), 4332-4343. DOI: 10.1021/acs.est.0c05471.
(20) Fillion, D.; Perrier, S.; Riva, M.; George, C.; Domine, F.; Couture, R.-M. Emission of Volatile Organic Compounds to the Atmosphere from Photochemistry in Thermokarst Ponds in Subarctic Canada. *ACS Earth and Space Chemistry* **2024**, *8* (3), 563-574. DOI: 10.1021/acsearthspacechem.3c00336.
(21) Yacovitch, T. I.; Lerner, B. M.; Canagaratna, M. R.; Daube, C.; Healy, R. M.; Wang, J. M.; Fortner, E. C.; Majluf, F.; Claflin, M. S.; Roscioli, J. R.; et al. Mobile Laboratory Investigations of Industrial Point Source Emissions during the MOOSE Field Campaign. *Atmosphere* **2023**, *14* (11), 1632.
(22) Sisco, E.; Forbes, T. P.; Staymates, M. E.; Gillen, G. Rapid analysis of trace drugs and metabolites using a thermal desorption DART-MS configuration. *Analytical Methods* **2016**, *8* (35), 6494-6499, 10.1039/C6AY01851C. DOI: 10.1039/C6AY01851C.
(23) Sisco, E.; Staymates, M. E.; Forbes, T. P. Optimization of confined direct analysis in real time mass spectrometry (DART-MS). *Analyst* **2020**, *145* (7), 2743-2750, 10.1039/D0AN00031K. DOI: 10.1039/D0AN00031K.
(24) Nudnova, M. M.; Zhu, L.; Zenobi, R. Active capillary plasma source for ambient mass spectrometry. *Rapid Communications in Mass Spectrometry* **2012**, *26* (12), 1447-1452. DOI: https://doi.org/10.1002/rcm.6242.
(25) Gyr, L.; Klute, F. D.; Franzke, J.; Zenobi, R. Characterization of a Nitrogen-Based Dielectric Barrier Discharge Ionization Source for Mass Spectrometry Reveals Factors Important for Soft Ionization. *Analytical Chemistry* **2019**, *91* (10), 6865-6871. DOI: 10.1021/acs.analchem.9b01132.
(26) Weber, M.; Wolf, J.-C.; Haisch, C. Effect of Dopants and Gas-Phase Composition on Ionization Behavior and Efficiency in Dielectric Barrier Discharge Ionization. *Journal of the American Society for Mass Spectrometry* **2023**, *34* (4), 538-549. DOI: 10.1021/jasms.2c00279.
(27) Wolf, J.-C.; Gyr, L.; Mirabelli, M. F.; Schaer, M.; Siegenthaler, P.; Zenobi, R. A Radical-Mediated Pathway for the Formation of [M + H]+ in Dielectric Barrier Discharge Ionization. *Journal of the American Society for Mass Spectrometry* **2016**, *27* (9), 1468-1475. DOI: 10.1007/s13361-016-1420-2.
(28) Song, Y.; Cooks, R. G. Atmospheric pressure ion/molecule reactions for the selective detection of nitroaromatic explosives using acetonitrile and air as reagents. *Rapid Communications in Mass Spectrometry* **2006**, *20* (20), 3130-3138. DOI: https://doi.org/10.1002/rcm.2714.
(29) Nilles, J. M.; Connell, T. R.; Stokes, S. T.; Dupont Durst, H. Explosives Detection Using Direct Analysis in Real Time (DART) Mass Spectrometry. *Propellants, Explosives, Pyrotechnics* **2010**, *35* (5), 446-451. DOI: 10.1002/prep.200900084.

(30) Forbes, T. P.; Sisco, E.; Staymates, M. Detection of Nonvolatile Inorganic Oxidizer-Based Explosives from Wipe Collections by Infrared Thermal Desorption—Direct Analysis in Real Time Mass Spectrometry. *Analytical Chemistry* **2018**, *90* (11), 6419-6425. DOI: 10.1021/acs.analchem.8b01037.
(31) *ASTM E2677 Limit of Detection Web Portal*. 2014. https://www-s.nist.gov/loda/ (accessed 20162016).
(32) Ewing, R. G.; Waltman, M. J.; Atkinson, D. A.; Grate, J. W.; Hotchkiss, P. J. The vapor pressures of explosives. *TrAC Trends in Analytical Chemistry* **2013**, *42*, 35-48. DOI: http://dx.doi.org/10.1016/j.trac.2012.09.010.
(33) Najarro, M.; Davila Morris, M. E.; Staymates, M. E.; Fletcher, R.; Gillen, G. Optimized thermal desorption for improved sensitivity in trace explosives detection by ion mobility spectrometry. *Analyst* **2012**, *137* (11), 2614-2622, 10.1039/C2AN16145A. DOI: 10.1039/C2AN16145A.
(34) Forbes, T. P.; Staymates, M.; Sisco, E. Broad spectrum infrared thermal desorption of wipe-based explosive and narcotic samples for trace mass spectrometric detection. *Analyst* **2017**, *142* (16), 3002-3010, 10.1039/C7AN00721C. DOI: 10.1039/C7AN00721C.
(35) Ewing, R. G.; Valenzuela, B. R.; Atkinson, D. A.; Wilcox Freeburg, E. D. Detection of Inorganic Salt Based Home Made Explosives (HME) by Atmospheric Flow Tube – Mass Spectrometry. *Analytical Chemistry* **2018**, *90* (13), 8086-8092. DOI: 10.1021/acs.analchem.8b01261.
(36) Yu, S.; Crawford, E.; Tice, J.; Musselman, B.; Wu, J.-T. Bioanalysis without Sample Cleanup or Chromatography: The Evaluation and Initial Implementation of Direct Analysis in Real Time Ionization Mass Spectrometry for the Quantification of Drugs in Biological Matrixes. *Analytical Chemistry* **2009**, *81* (1), 193-202. DOI: 10.1021/ac801734t.
(37) Weinmann, W.; Stoertzel, M.; Vogt, S.; Wendt, J. Tune compounds for electrospray ionisation/in-source collision-induced dissociation with mass spectral library searching. *Journal of Chromatography A* **2001**, *926* (1), 199-209. DOI: https://doi.org/10.1016/S0021-9673(01)01066-4.
(38) Musah, R. A.; Cody, R. B.; Domin, M. A.; Lesiak, A. D.; Dane, A. J.; Shepard, J. R. E. DART–MS in-source collision induced dissociation and high mass accuracy for new psychoactive substance determinations. *Forensic Science International* **2014**, *244*, 42-49. DOI: https://doi.org/10.1016/j.forsciint.2014.07.028.
(39) Forbes, T. P.; Sisco, E. In-source collision induced dissociation of inorganic explosives for mass spectrometric signature detection and chemical imaging. *Analytica Chimica Acta* **2015**, *892*, 1-9. DOI: http://dx.doi.org/10.1016/j.aca.2015.06.008.
(40) Forbes, T. P.; Verkouteren, J. R. Forensic Analysis and Differentiation of Black Powder and Black Powder Substitute Chemical Signatures by Infrared Thermal Desorption-DART-MS. *Analytical Chemistry* **2019**, *91* (1), 1089-1097, Article. DOI: 10.1021/acs.analchem.8b04624.
(41) Moorthy, A. S.; Tennyson, S. S.; Sisco, E. Updates to the Inverted Library Search Algorithm for Mixture Analysis. *Journal of the American Society for Mass Spectrometry* **2022**, *33* (7), 1260-1266. DOI: 10.1021/jasms.2c00090.
(42) *United States Bomb Data Center (USBDC) Explosives Incident Report (EIR)*. https://www.atf.gov/resource-center/data-statistics (accessed March 4, 2024).
(43) Crawford, C. L.; Boudries, H.; Reda, R. J.; Roscioli, K. M.; Kaplan, K. A.; Siems, W. F.; Hill, H. H. Analysis of Black Powder by Ion Mobility−Time-of-Flight Mass Spectrometry. *Analytical Chemistry* **2010**, *82* (1), 387-393. DOI: 10.1021/ac902168a.
(44) Krauss, S. T.; Forbes, T. P.; Jobes, D. Inorganic oxidizer detection from propellants, pyrotechnics, and homemade explosive powders using gradient elution moving boundary electrophoresis. *Electrophoresis* **2021**, *42* (3), 279-288. DOI: https://doi.org/10.1002/elps.202000279.
(45) Sisco, E.; Najarro, M.; Samarov, D.; Lawrence, J. Quantifying the stability of trace explosives under different environmental conditions using electrospray ionization mass spectrometry. *Talanta* **2017**, *165*, 10-17. DOI: https://doi.org/10.1016/j.talanta.2016.12.029.
(46) Bachmann, W. E.; Sheehan, J. C. A New Method of Preparing the High Explosive RDX. *J. Am. Chem. Soc.* **1949**, *71* (5), 1842-1845. DOI: 10.1021/ja01173a092.